A vapor–liquid phase equilibrium model for binary CO_2–H_2O and CH_4–H_2O systems above 523 K for application to fluid inclusions

Shide Mao [a], Zhenhao Duan [b,*], Wenxuan Hu [c]

[a] *State Key Laboratory of Geological Processes and Mineral Resources, and School of Earth Sciences and Resources, China University of Geosciences, Beijing 100083, China*
[b] *Key Laboratory of the Earth's Deep Interior, Institute of Geology and Geophysics, Chinese Academy of Sciences, 19 Beitucheng Xilu Rd, Beijing 100029, China*
[c] *Nanjing University, School of Earth Sciences and Engineering, State Key Laboratory for Mineral Deposits Research, Nanjing 210093, China*

ARTICLE INFO

ABSTRACT

Accurate prediction of both volumetric and vapor–liquid phase equilibria of binary CO_2–H_2O and CH_4–H_2O mixtures with a single equation of state proves to be difficult. In this study we use an activity–fugacity model to predict the vapor–liquid phase equilibria above 523 K and adapt a Helmoholtz model to calculate volumetric properties of these two binary systems. The average deviations of water content in the vapor phase from experimental data are 3.25% and 3.19% for the CO_2–H_2O and CH_4–H_2O mixtures, respectively, and the average deviations of gas solubility in liquid phase from experimental data are 4.29% and 3.50%, respectively. The model can find wide applications, and an example is given for the analysis of fluid inclusions in geochemistry.

© 2009 Published by Elsevier B.V.

1. Introduction

CO_2–H_2O and CH_4–H_2O mixtures are typical geological fluids in the Earth's crust. Vapor–liquid phase equilibria [1–4] and volumetric (*PVTx*) properties [5–7] of the two systems are fundamental in the quantitative interpretation of boiling, immiscibility, gas solubility, and fluid migration, and also in the studies of fluid inclusions [8–12].

Due to highly non-ideal mixing properties of the binary CO_2–H_2O and CH_4–H_2O fluid mixtures, it is difficult to predict both the phase equilibria and volumetric properties simultaneously with an equation of state within experimental uncertainty over a large temperature–pressure region, such as 273–647 K for vapor–liquid equilibria, or 273–1273 K for volume. However, it is possible to use an equation of state to calculate the volume of these binary mixtures, and use another model to predict the vapor–liquid phase equilibria with different parameters for the vapor and liquid phases. Previously, Duan and Sun [2] developed a model for calculating CO_2 solubility in pure water from 273 to 533 K and from 1 to 2000 bar and Duan and Mao [3] presented a model for calculating the vapor–liquid phase equilibria of the CH_4–H_2O system from 273 to 523 K and from 1 to 2000 bar. However, high temperature (above 523 K) phase equilibrium models of these two systems are still lacking.

In this study, phase equilibrium models at high temperatures between 523 and 623 K and pressures up to 1500 bar (or P_c, the critical pressure, lower than 1500 bar) are established. First, competitive volumetric (*PVTx*) models for the CO_2–H_2O and CH_4–H_2O mixtures are briefly reviewed. Then it is shown that by combining the vapor–liquid phase equilibrium models reviewed and volumetric models that homogenization pressure, homogenization volume (or density) and isochores at given homogenization temperature and composition can be applied to the interpretation of microthermometric observations of fluid inclusions in minerals containing CO_2–H_2O and CH_4–H_2O.

2. Vapor–liquid phase equilibria of the binary CO_2–H_2O and CH_4–H_2O mixtures at high temperatures

2.1. Review of experimental data above 523 K

There are many experimental data on the vapor–liquid phase equilibria of the binary CO_2–H_2O and CH_4–H_2O mixtures below 523 K, and they are reviewed by Duan and Sun [2] and Duan and Mao [3]. However, there are a few experimental data above 523 K. In this study, we focus on the temperature range from 523 to 647 K.

2.1.1. CO_2–H_2O mixture

Over 270 measurements of the CO_2 solubility in pure water have been reported [13–21], covering a temperature range of 523–623 K. A few data points of Drummond [19] measured during the pres-

* Corresponding author. Tel.: +86 10 82998377.
  E-mail address: duanzhenhao@gmail.com (Z. Duan).

Table 1
Parameters of Eq. (5).

	CO_2–H_2O	CH_4–H_2O
c_1	$-0.14103545D+05$	$0.20222024D+05$
c_2	$0.16583148D+02$	$-0.24120165D+02$
c_3	$0.53326776D+07$	$-0.75058093D+07$
c_4	$-0.73088779D-02$	$0.10747756D-01$
c_5	$-0.75551470D+09$	$0.10421822D+10$
c_6	$-0.32657539D-01$	$-0.16556694D-01$
c_7	$0.16982222D-04$	$0.16641012D-04$
c_8	$0.12515020D+02$	$0.47915976D+01$
c_9	$0.49580878D-09$	$-0.18148280D-09$

sure increasing process are not consistent with those measured in the pressure decreasing process. The deviation between them is 8–15%. The CO_2 solubilities from Todheide and Franck [17] are overestimated due to systematic analytical error, as pointed out by Blencoe [21], and their data are inconsistent with others. Therefore, all CO_2 solubility data points listed above are used in the parameterization, except those of Drummond [19] and Todheide and Franck [17].

About 180 measurements of water content in the vapor phase of the CO_2–H_2O system have been reported [13,16,17,20,21]. However, the data points from Todheide and Franck [17] are questionable due to systematic analytical error, and their data are excluded from our parameterization, which covers a temperature range from 523 to 623 K and pressure up to 1500 bar.

2.1.2. CH_4–H_2O mixture

Above 523 K, there are only two data sets for the vapor–liquid phase equilibrium of CH_4–H_2O system [22,23]. For the CH_4 solubility in water, the data of Sultanov et al. [22] are not consistent with those of Price [23]. However, the data points of Price [23] at low temperatures are consistent with other measurements. Experimental data can be plotted on the same isobaric composition–temperature or isothermal composition–pressure figure, from which consistency of experimental data can be seen. Therefore, the data points of Price [23] are used in the parameterization with temperature up to 627 K and pressure to about 2000 bar. As for the water content of the CH_4–H_2O mixture at high temperatures, only Sultanov et al. [22] made experimental measurements (48 data points), and their data are included in the parameterization of our model.

2.2. Phase equilibrium model as a function of temperature and pressure

2.2.1. Gas solubility in water

CO_2 (or CH_4) solubility in aqueous solutions depends on the balance between the chemical potential of CO_2 (or CH_4) in the liquid phase μ_i^l (i = CO_2 or CH_4 of the binary CO_2–H_2O or CH_4–H_2O mixtures, respectively) and that in the vapor phase μ_i^v. The chemical potential can be written in terms of fugacity in the vapor phase and activity in the liquid phase:

$$\mu_i^v(T,P) = \mu_i^{v(0)}(T) + RT\ \ln f_i(T,P)$$
$$= \mu_i^{v(0)}(T) + RT\ \ln y_iP + RT\ln \varphi_i(T,P) \quad (1)$$

$$\mu_i^l(T,P) = \mu_i^{l(0)}(T,P) + RT\ \ln a_i(T,P)$$
$$= \mu_i^{l(0)}(T,P) + RT\ \ln m_i + RT\ \ln \gamma_i(T,P) \quad (2)$$

where $\mu_i^{l(0)}$, the standard chemical potential of i in liquid, is defined as the chemical potential in hypothetically ideal solution of unit molality [24] and $\mu_i^{v(0)}$, the standard chemical potential in vapor, is the hypothetical ideal gas chemical potential when the pressure is set to 1 bar, y_i is mole fraction of i in the vapor phase, and φ_i is the fugacity coefficient of i in vapor phase.

For phase equilibrium $\mu_i^l = \mu_i^v$, and one obtains:

$$\ln \frac{y_iP}{m_i} = \frac{\mu_i^{l(0)}(T,P) - \mu_i^{v(0)}(T)}{RT} + \ln\ \gamma_i(T,P) - \ln \varphi_i(T,P) \quad (3)$$

where the fugacity coefficient of i in gaseous mixtures is generally calculated from an equation of state (EOS). An EOS is not only a function of temperature, pressure and volume or density, but also a non-linear function of composition. Obtaining accurate H_2O content in vapor phase is difficult both experimentally and theoretically (solving the non-linear EOS for vapor composition). Because the fugacity coefficient of i in gaseous mixtures differs little from that of pure i in the studied region and the little difference from this approximation is canceled in the later parameter fitting, therefore, $\ln \varphi_i$ can be approximated from the EOS of pure CO_2 or CH_4 [25] (see Appendix). y_i, the mole fraction of i in the vapor phase, is calculated from

$$y_i = 1 - y_{H_2O} = \frac{P - P_{H_2O}}{P} \quad (4)$$

Table 2
Calculated composition deviations from experimental data at vapor–liquid phase equilibria.

References	T (K)	P (bar)	Nd	AAD (%)	MAD (%)
CO_2 solubility in water in CO_2–H_2O mixture					
[13]	523.15–603.15	98–490	47	3.06	8.06
[14]	534.15–607.17	71.49–198.70	9	2.61	3.90
[15]	523.15–623.15	100–1400	17	5.25	16.94
[16]	523.15–623.15	100–1500	71	5.10	19.33
[20]	573.15	276.1–515.2	3	6.57	16.08
[21]	623.15	209.7–296	4	8.33	21.71
Water content in CO_2–H_2O mixture at phase equilibria					
[20]	573.15	516.5–566.1	3	5.93	11.7
[16]	523.15–623.15	100–1500	71	3.47	16.22
[13]	523.15–603.15	196–490	30	2.87	9.05
[21]	623.15	187–298.9	6	1.36	3.74
CH_4 solubility in water in CH_4–H_2O mixture					
[23]	507–627	81.1–1972.6	45	3.50	10.85
Water content in CH_4–H_2O mixture at phase equilibria					
[22]	523.2633.2	98.1–1132.7	48	3.19	10.14

AAD: average absolute deviations calculated from this model; MAD: maximal absolute deviations calculated from this model; Nd: number of data points.
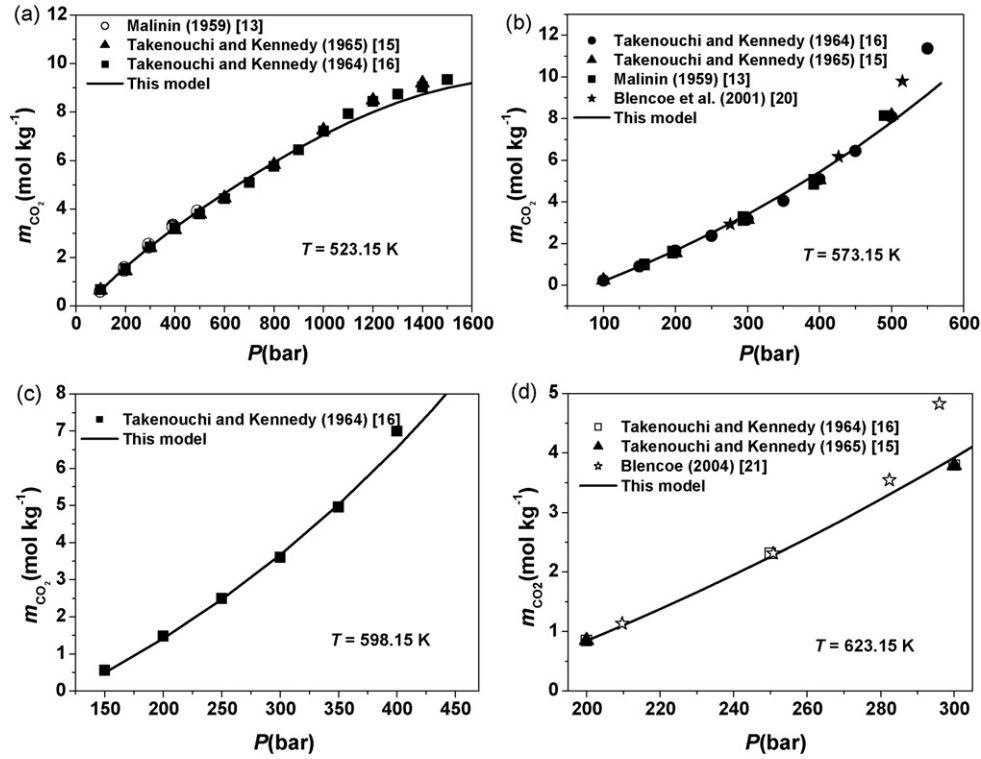
Fig. 1. CO_2 solubility in pure water at high temperatures: according to Blencoe [21], the critical pressures at 573.15, 598.15 and 623.15 K are 568.69, 469.49 and 301.92 bar, respectively.
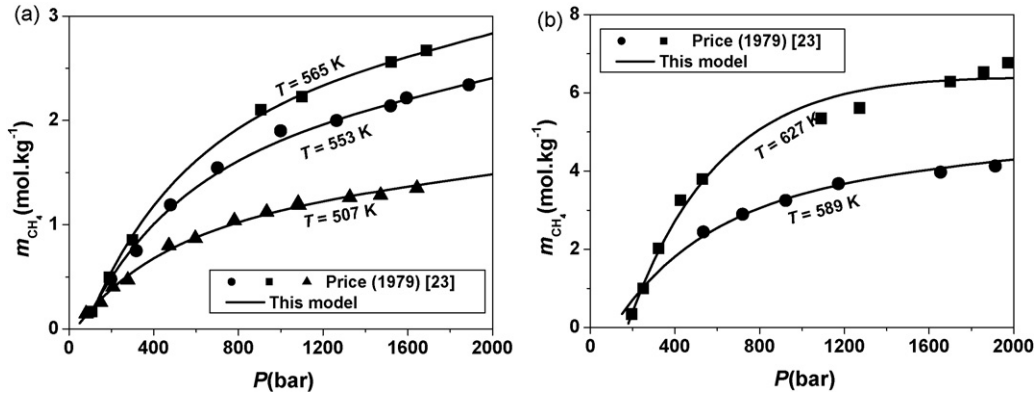

Fig. 2. CH_4 solubility in pure water at high temperatures.

where the partial pressure of water in vapor, P_{H_2O}, is approximated as the saturated pressure of pure water as that in our previous studies [26,27], and this approximation will lead to errors (up to 5%) for $\mu_i^{l(0)}/RT$ and $\ln \gamma_i^l$. However, these errors tend to cancel out to a large extent in the parameterization and have little effect on the calculated gas solubility in water because in the calculation of gas solubility, only the chemical potential difference between liquid and vapor is important. In fitting to the experimental solubility

data, the error in the vapor phase can be transferred to the empirical parameters of the liquid phase. And the subsequent error in the liquid phase calculation is negligible. The saturated pressure of pure water here is from the equation of Wagner and Pruss [28].

$(\mu_i^{l(0)}(T, P) - \mu_i^{v(0)}(T))/RT + \ln \gamma_i(T, P)$ in Eq. (3) is a function of temperature and pressure and can be calculated from the following equation:

$$\frac{\mu_i^{l(0)}(T, P) - \mu_i^{v(0)}(T)}{RT} + \ln \gamma_i(T, P) = c_1 + c_2 T + \frac{c_3}{T} + c_4 T^2 + \frac{c_5}{T^2}$$

$$+ c_6 P + c_7 PT + \frac{c_8 P}{T} + c_9 P^2 T \quad (5)$$

where c_1–c_9 (Table 1) are obtained by regressing the reliable gas solubility data in the liquid phase for the binary CO_2–H_2O and CH_4–H_2O systems, as described in Section 2.1.

With these parameters, the CO_2 or CH_4 solubility in pure water above 523 K can be calculated; the average deviations from exper-

Table 3
Parameters of Eq. (7).

	CO_2–H_2O	CH_4–H_2O
a_1	$0.15884702D-01$	$0.47258673D-01$
a_2	$-0.22882000D-05$	$0.12938130D-05$
a_3	$-0.13944627D-04$	$-0.46620644D-04$
a_4	$-0.61510488D+01$	$-0.12663219D+02$
a_5	$0.18428359D-02$	$-0.95871477D-04$
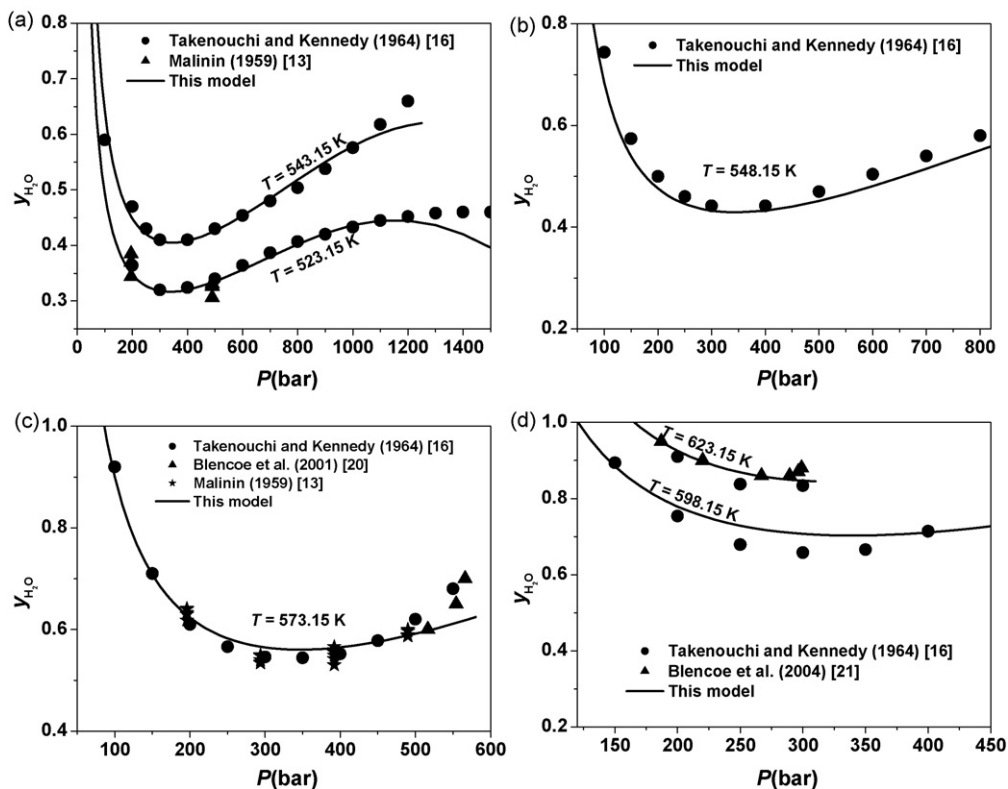
Fig. 3. Water content of the vapor phase for CO_2–H_2O system at high temperatures: y_{H_2O} is mole fraction of water in vapor phase; according to Blencoe [21], the critical pressures at 543.15, 548.15, 573.15, 598.15 and 623.15 K are 1253.00, 995.11, 568.69, 469.49 and 301.92 bar, respectively.

imental data are 4.29% and 3.50% for the binary CO_2–H_2O and CH_4–H_2O mixtures, respectively, and they are within experimental uncertainties. Table 2 shows the average and maximal deviations of the model from each data set. Figs. 1 and 2 show the comparisons

between the experimental results and model predictions. As can be seen in Figs. 1 and 2, the molality of CO_2 or CH_4 in water increases with pressures at given temperatures, and the experimental gas solubility data are accurately reproduced by Eq. (5) except in the
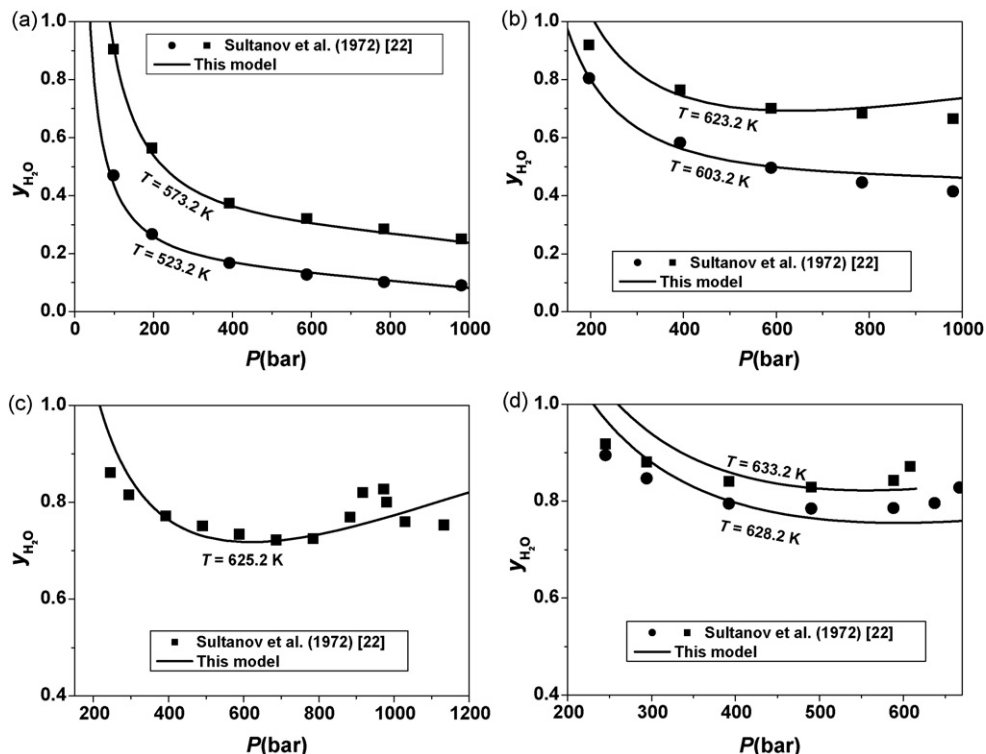

Fig. 4. Water content of the vapor phase for CH_4–H_2O system at high temperatures: y_{H_2O} is mole fraction of water in vapor phase.

Table 4
Models adopted for the CO_2–H_2O and CH_4–H_2O fluid inclusions.

	CO_2–H_2O	T (K)	P (bar)	CH_4–H_2O	T (K)	P (bar)
Vapor–liquid phase equilibria models	[2]	273–523	<2,000	[3]	273–523	<2,000
	This model	523–623	<1,500	This model	523–623	<2,000
Volumetric models	[5]	273–1273	<10,000	[6]	273–1273	<10,000
	[43]	1273–2573	<100,000			

critical region, where deviations increase to over 10%. Eq. (5) can be used to satisfactorily calculate homogenization pressure of fluid inclusions.

2.2.2. Water content in vapor phase

Water content of the binary CO_2–H_2O or CH_4–H_2O mixtures in the vapor phase above 523 K can be estimated using the following equation:

$$y_{H_2O} = \frac{\gamma_{H_2O} x_{H_2O} P^S_{H_2O}}{\varphi_{H_2O} P} \exp\left(\frac{v^l_{H_2O}(P - P^S_{H_2O})}{RT}\right) \quad (6)$$

where y_{H_2O} denotes the mole fraction of water in the vapor phase, x_{H_2O} is the mole fraction of H_2O in the liquid phase, γ_{H_2O} is the activity coefficient of water in the liquid phase, $P^S_{H_2O}$, the saturation pressure (bar) of water calculated from the correlation of Wagner and Pruss [28], $v^l_{H_2O}$ is the molar volume of liquid water ($cm^2\,mol^{-1}$) approximated as the saturated liquid phase volume of water calculated from the equation of Wagner and Pruss [28], and φ_{H_2O} refers to the fugacity coefficient of water in the vapor phase.

The remaining parameters of Eq. (6) for the calculation of water content in the vapor phase are $\varphi_{H_2O}/\gamma_{H_2O} x_{H_2O}$, which are functions of temperature and pressure and can be calculated from the follow-
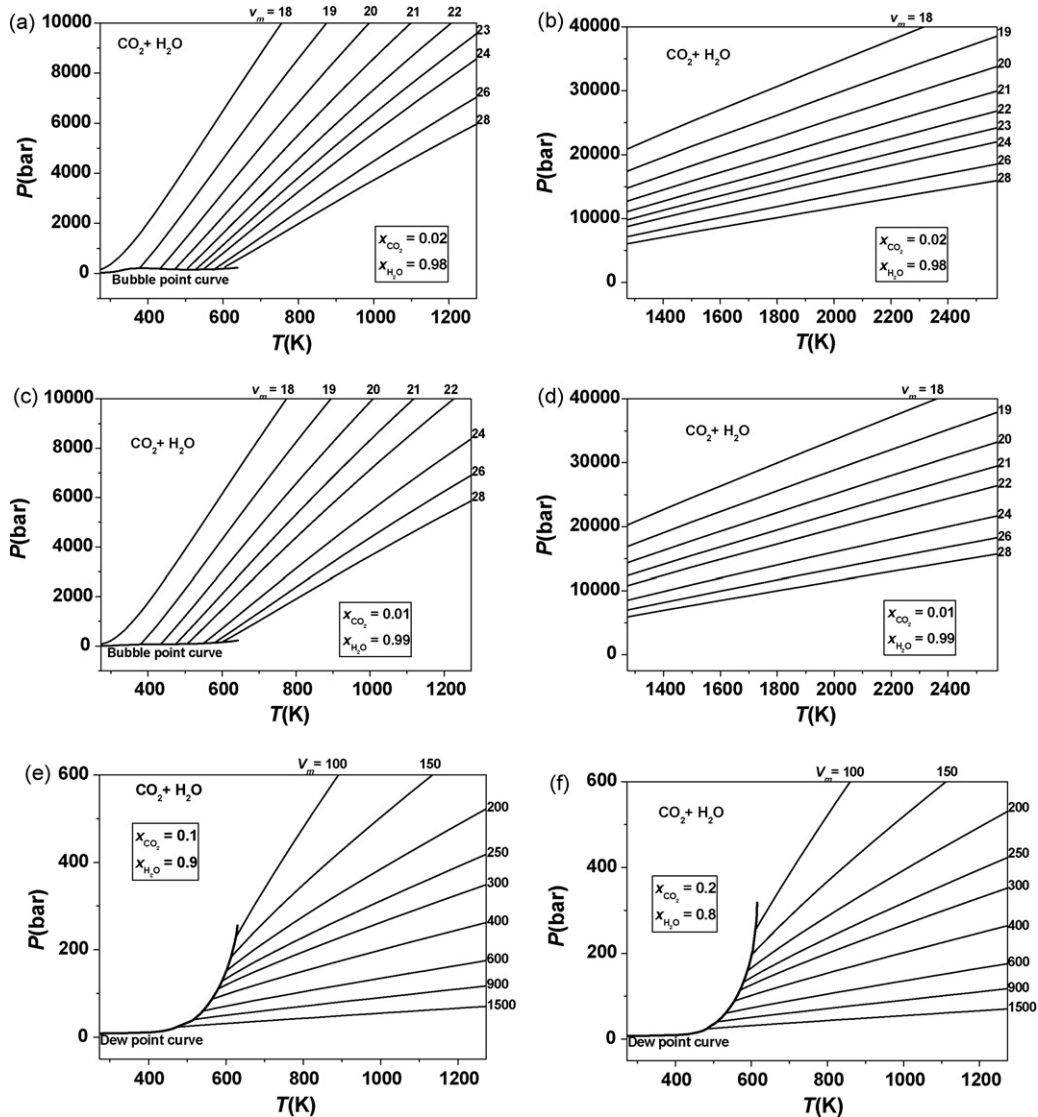

Fig. 5. Isochores of CO_2–H_2O system: bubble point curve and dew point curve above 523 K are from this model, and those below 523 K are from the model of Duan and Sun [2]; isochores between 273 and 1273 K are from the *PVTx* model of Paulus and Penoncello [5], and isochores between 1273 and 2573 K are from the volume model of Duan and Zhang [43]; unit of V_m is $cm^3\,mol^{-1}$.
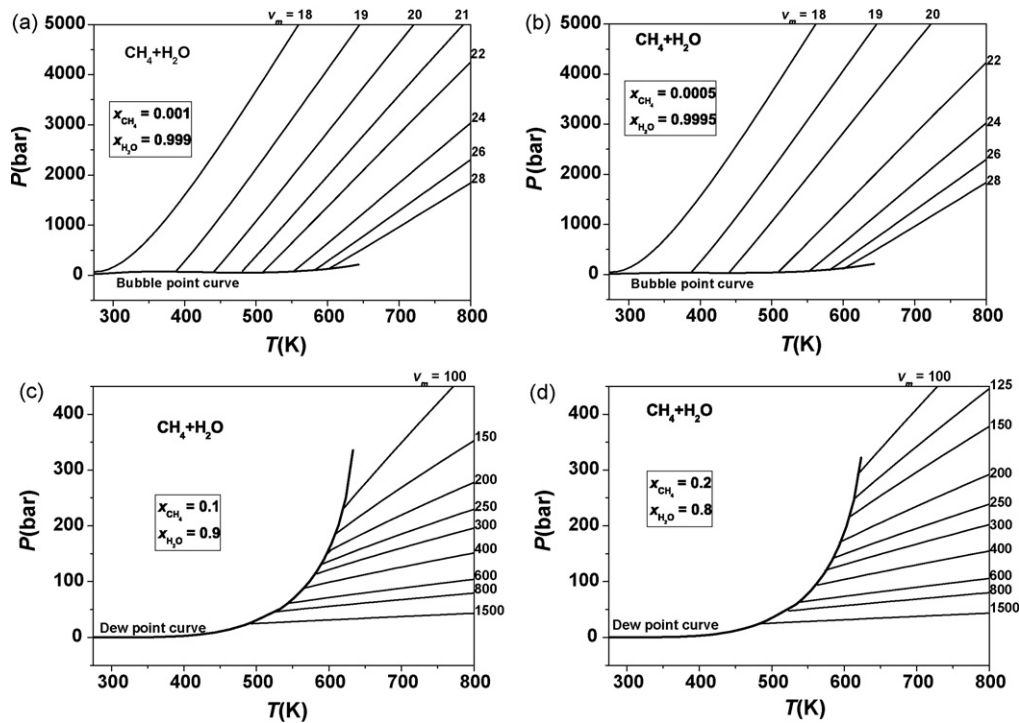
Fig. 6. Isochores of CH_4–H_2O system: bubble point curve and dew point curve above 523 K are from this model, and those below 523 K are from the model of Duan and Mao [3]; isochores are from the *PVTx* model of Kunz et al. [6]; unit of V_m is $cm^3\ mol^{-1}$.

ing semi-empirical equation:

$$\frac{\varphi_{H_2O}}{\gamma_{H_2O}x_{H_2O}} = \exp\left(a_1(P - P^S_{H_2O}) + a_2(P - P^S_{H_2O})^2 + a_3(P - P^S_{H_2O})T\right.$$

$$\left. + \frac{a_4(P - P^S_{H_2O})}{T} + \frac{a_5(P - P^S_{H_2O})^2}{T}\right) \tag{7}$$

where a_1–a_5 (Table 3) are obtained by regressing the water content data in the vapor phase discussed above for the CO_2–H_2O or CH_4–H_2O systems. The water content in the vapor phase can be reproduced by Eqs. (6) and (7), as shown by Figs. 3 and 4. Table 2 also shows the average and maximal deviations of the water content from each experimental set. The average deviations of the water content from experimental data in the vapor phase are 3.25% and 3.19% for the CO_2–H_2O and CH_4–H_2O mixtures, respectively. When total pressure P approaches the saturation pressure of pure

water, y_{H_2O} approaches 1. As CO_2–H_2O or CH_4–H_2O fluid inclusions homogenize to the vapor phase at high temperatures, homogenization pressures can be obtained from Eqs. (6) and (7) by an iterative method.

3. Volumetric (*PVTx*) models for the binary CO_2–H_2O and CH_4–H_2O mixtures

There are five types of models for the calculation of volumetric properties of the CO_2–H_2O and CH_4–H_2O systems: (1) equations of state (EOS) [5–7,29–43]; (2) liquid density models [44–47]; (3) partial molar volume models [48–51]; (4) apparent molar volume models [45,52–56]; and (5) excess volume models [29,57–59]. Each model has its strength and weakness. For the binary CO_2–H_2O and CH_4–H_2O fluid mixtures, Helmholtz energy equations of state are the best among these five types of models. These equations of state can not only reproduce the existing

Table 5
Calculated results of the CO_2–H_2O and CO_2 fluid inclusions.

	P–T relation					
	T (K)	*P* (bar)	*T* (K)	*P* (bar)	*T* (K)	*P* (bar)
CO_2–H_2O inclusion (V + L − L)						
Th = 573 K	573.00	143.14	823.15	2773.35	1073.15	5295.87
x_{CO_2} = 0.015	623.15	660.04	873.15	3292.64	1123.15	5777.38
Ph = 143.14 bar	673.15	1187.73	923.15	3804.93	1173.15	6251.42
Vh = 25.68 cm^3 mol	723.15	1718.60	973.15	4309.69	1223.15	6718.24
Dh = 0.7167 g cm^{-3}	773.15	2248.09	1023.15	4806.67	1273.15	7178.10
CO_2 inclusion (V + L − L)	295	59.82	600	1359.52	950	2715.17
Th = 295 K	300	79.82	650	1562.64	1000	2898.03
Ph = 59.82 bar	350	293.4	700	1762.28	1050	3078.71
Vh = 58.48 cm^3 mol	400	511.73	750	1958.64	1100	3257.35
Dh = 0.7526 g cm^{-3}	450	728.53	800	2151.90	1150	3468.46
	500	942.41	850	2342.29	1200	3649.73
	550	1152.79	900	2529.98	1250	3829.62

Note: Th, Ph, Vh and Dh denote homogenization temperature, pressure, mole volume and density, respectively; "V + L = L" denotes homogenization to liquid phase; x_{CO_2} is mole fraction CO_2 in CO_2–H_2O mixture. Used models or equations of state are the same as those in Fig. 7.
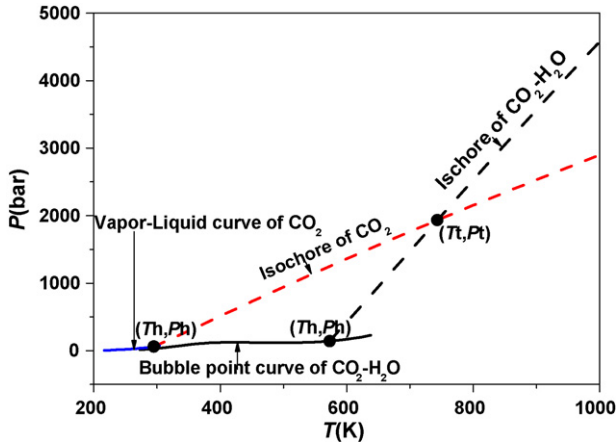
Fig. 7. Isochores of CO_2–H_2O and CO_2 fluid inclusions in Sanja lode gold deposit, Jiaodong peninsula of eastern China: Th and Ph denote homogenization temperature and pressure, respectively, values see Table 5; Tt and Pt denote trapped temperature and pressure, respectively. The two inclusions homogenize to liquid phase. Bubble point curve of CO_2–H_2O fluid above 523 K is from this model, and that below 523 K is from the model of Duan and Sun [2]. Isochores of CO_2–H_2O fluid are from the *PVTx* model of Paulus and Penoncello [5]. Vapor–liquid curve and isochores of CO_2 fluid are from equation of state of Span and Wagner [63]. Calculated Tt = 743.32 K and Pt = 1932.57 bar.

data, but also can be extrapolated to predict volumetric properties in the high temperature–pressure region with reasonable trend as pointed out by Span and Wagner [60], which can find wide applications in the study of fluid inclusions. Kunz et al. [6] and Paulus and Penoncello [5] respectively developed an equation of state in terms of Helmholtz energy for the volume of the CO_2–H_2O fluid mixture. It should be noted that when CO_2 is dissolved in liquid water up to 473 K, the density of solutions will increase [61]. But the volumetric model of Kunz et al. [6] fails in this aspect. Therefore, the equation of state of Paulus and Penoncello [5] is chosen for calculating the volume of the CO_2–H_2O fluid mixture, covering the T–P range of 273–1273 K and 1–10,000 bar, where equations of pure H_2O are from Wagner and Pruß [62] and equations of pure CO_2 are from Span and Wagner [63]. Above 1273 K, the equation of state of Duan and Zhang [43] based on the data of molecular dynamics simulations is used to calculate isochores of the CO_2–H_2O fluid mixtures. The equation of state of Kunz et al. [6] is adopted for calculating the volume of the CH_4–H_2O fluid mixture.

4. Application in fluid inclusions

The model presented here can find wide applications, such as predicting fluid boiling of hydrothermal fluids, calculating CO_2 solubility related to CO_2 geological sequestration, and applying to the study of fluid inclusions. Applications to fluid inclusions are discussed below.

The vapor–liquid phase equilibrium models from 273 to 623 K and volumetric models from 273 to 2573 K adopted for the study of fluid inclusions are listed in Table 4. Usually, temperature and composition of the fluid inclusions can be obtained from microthermometric observations, but homogenization density (volume), homogenization pressure, and isochores must be acquired from thermodynamic models, as demonstrated in this study by combining the vapor–liquid phase equilibrium and volumetric models (Figs. 5 and 6). From Figs. 5 and 6, it can be seen that isochores in liquid phase are a bit curved below 400 K and 1000 bar, but are almost linear at higher temperatures.

Here an actual example is given to illustrate how to use this model for the study of fluid inclusions. There are two kinds of original fluid inclusions in Sanja lode gold deposit, Jiaodong peninsula

of eastern China: one is CO_2–H_2O inclusion with CO_2 mole fraction of 0.015, and total homogenization temperature $Th(CO_2$–$H_2O)$ is 573 K; the other is pure CO_2 inclusion, and homogenization temperature $Th(CO_2)$ is 295 K. The two kinds of inclusion finally homogenize to liquid phase. Based on these microthermometric data, corresponding homogenization pressure (density or volume) and isochores of CO_2–H_2O mixture is obtained from the phase equilibrium and volumetric models. Saturation curve and isochores of pure CO_2 fluid are from equation state of Span and Wagner [63]. Calculated results of the CO_2–H_2O and CO_2 fluid inclusions are listed in Table 5. Isochores are plotted in Fig. 7, from which trapped temperature (Tt) and pressure (Pt) of ore fluids are determined: Tt = 743.32 K and Pt = 1932.57 bar. Therefore, temperature–pressure conditions of the trapped ore fluids are obtained from the model.

5. Conclusions

A phase equilibrium model of the binary CO_2–H_2O and CH_4–H_2O fluid mixtures between 523 and 623 K and pressures up to 1500 bar (or the critical pressure, lower than 1500 bar) are established within or about experimental uncertainties. Volumetric (*PVTx*) models for the CO_2–H_2O and CH_4–H_2O mixtures are reviewed, and the competitive volumetric models of the CO_2–H_2O [5,43] and CH_4–H_2O [6] fluid mixtures are adapted. Results of this study, together with previous phase equilibrium models of Duan and Sun [2] and Duan and Mao [3], and the volumetric models of the CO_2–H_2O [5,43] and CH_4–H_2O [6] mixtures are applied to the fluid inclusions, such that homogenization pressure, homogenization volume or density, and isochores at given homogenization temperatures and compositions can be obtained. Online calculations can be made on: http://www.geochem-model.org/research/fluidinc.

Appendix A. Appendix

Equation of state for pure CO_2 and CH_4

$$Z = \frac{P_r V_r}{T_r} = 1 + \frac{a_1 + a_2/T_r^2 + a_3/T_r^3}{V_r} + \frac{a_4 + a_5/T_r^2 + a_6/T_r^3}{V_r^2}$$
$$+ \frac{a_7 + a_8/T_r^2 + a_9/T_r^3}{V_r^4} + \frac{a_{10} + a_{11}/T_r^2 + a_{12}/T_r^3}{V_r^5}$$
$$+ \frac{a_{13}}{T_r^3 V_r^2} \left(a_{14} + \frac{a_{15}}{V_r^2} \right) \exp \left(-\frac{a_{15}}{V_r^2} \right) \tag{A1}$$

$$P_r = \frac{P}{P_c}; \quad T_r = \frac{T}{T_c} \tag{A2}$$

$$V_r = \frac{V}{V_c}; \quad V_c = \frac{RT_c}{P_c} \tag{A3}$$

where P_r, T_r and V_r are reduced pressure, temperature and volume, respectively; P_c and T_c are critical pressure and critical temperature, respectively; R is universal gas constant (83.14472 bar cm^3 K^{-1} mol^{-1}); V is molar volume. Note that V_c is not the real critical volume. The parameters of the EOS are referred to Duan et al. [25]. Critical properties of CO_2 are: T_c = 304.2 K;

Table A1
Fugacity coefficient comparison for pure CO_2 and CH_4.

T (K)	P (bar)			
	100	250	500	1000
CO_2				
523	0.951 (0.947)	0.898 (0.890)	0.868 (0.860)	0.970 (0.962)
573	0.973 (0.968)	0.947 (0.938)	0.943 (0.934)	1.065 (1.058)
623	0.988 (0.984)	0.980 (0.972)	0.997 (0.988)	1.134 (1.129)
CH_4				
523	1.008 (1.008)	1.034 (1.035)	1.117 (1.121)	1.413 (1.428)
573	1.016 (1.016)	1.051 (1.052)	1.139 (1.145)	1.426 (1.444)
623	1.021 (1.022)	1.061 (1.064)	1.153 (1.161)	1.428 (1.450)

Note: The first value of fugacity coefficient is calculated from equation of state of Duan et al. [25]; the second value of fugacity coefficient in parentheses is calculated from equation of state NIST recommended: equation of state of Span and Wagner [63] is for CO_2 and equation of state of Setzmann and Wagner [64] is for CH_4.

$P_c = 73.825$ bar; the critical properties of CH_4 are: $T_c = 190.6$ K; $P_c = 46.41$ bar. Fugacity coefficient of pure CO_2 or CH_4 can be derived from Eq. (A1):

$$\ln \varphi(T, P) = Z - 1 - \ln Z + \frac{a_1 + a_2/T_r^2 + a_3/T_r^3}{V_r} + \frac{a_4 + a_5/T_r^2 + a_6/T_r^3}{2\ V_r^2}$$

$$+ \frac{a_7 + a_8/T_r^2 + a_9/T_r^3}{4\ V_r^4} + \frac{a_{10} + a_{11}/T_r^2 + a_{12}/T_r^3}{5\ V_r^5}$$

$$+ \frac{a_{13}}{2\ T_r^3 a_{15}} \left[a_{14} + 1 - \left(a_{14} + 1 + \frac{a_{15}}{V_r^2} \right) \exp\left(-\frac{a_{15}}{V_r^2} \right) \right] \tag{A4}$$

Fugacity coefficients of pure CO_2 or CH_4 from equation of state of Duan et al. [25] are compared with those from equations of state NIST recommended (Table A1): EOS of Span and Wagner [63] is for CO_2 and EOS of Setzmann and Wagner [64] is for CH_4. It can be seen that the calculated results from these equations are in good agreement. However, equation of state of Duan et al. [25] is simple and thus is used in this study.

References

[1] E. Perfetti, R. Thiery, J. Dubessy, Equation of state taking into account dipolar interactions and association by hydrogen bonding. II. Modelling liquid–vapour equilibria in the $H_2O–H_2S$, $H_2O–CH_4$ and $H_2O–CO_2$ systems, Chemical Geology 251 (2008) 50–57.

[2] Z. Duan, R. Sun, An improved model calculating CO_2 solubility in pure water and aqueous NaCl solutions from 273 to 533 K and from 0 to 2000 bar, Chemical Geology 193 (2003) 257–271.

[3] Z. Duan, S. Mao, A thermodynamic model for calculating methane solubility, density and gas phase composition of methane-bearing aqueous fluids from 273 to 523 K and from 1 to 2000 bar, Geochimica et Cosmochimica Acta 70 (2006) 3369–3386.

[4] L.W. Diamond, N.N. Akinfiev, Solubility of CO_2 in water from −1.5 to 100 °C and from 0.1 to 100 MPa: evaluation of literature data and thermodynamic modelling, Fluid Phase Equilibria 208 (2003) 265–290.

[5] M.E. Paulus, S.G. Penoncello, Correlation for the carbon dioxide and water mixture based on the Lemmon–Jacobsen mixture model and the Peng–Robinson equation of state, International Journal of Thermophysics 27 (2006) 1373–1386.

[6] O. Kunz, R. Klimeck, W. Wagner, J. M, The GERG-2004 wide-range equation of state for natural gases and other mixtures, Publishing House of the Association of German Engineers, 2007.

[7] J.S. Gallagher, R. Crovetto, J.M.H.L. Sengers, The thermodynamic behavior of the $CO_2–H_2O$ system from 400 to 1000 K, up to 100 MPa and 30% mole fraction of CO_2, Journal of Physical and Chemical Reference Data 22 (1993) 431–513.

[8] C.J. Bray, E.T.C. Spooner, Fluid inclusion volatile analysis by gas-chromatography with photoionization micro-thermal conductivity detectors—applications to magmatic MoS_2 and other $H_2O–CO_2$ and $H_2O–CH_4$ fluids, Geochimica et Cosmochimica Acta 56 (1992) 261–272.

[9] J. Dubessy, A. Moissette, R.J. Bakker, J.D. Frantz, Y.G. Zhang, High-temperature Raman spectroscopic study of $H_2O–CO_2–CH_4$ mixtures in synthetic fluid inclusions: first insights on molecular interactions and analytical implications, European Journal of Mineralogy 11 (1999) 23–32.

[10] D. Guillaume, S. Teinturier, J. Dubessy, J. Pironon, Calibration of methane analysis by Raman spectroscopy in $H_2O–NaCl–CH_4$ fluid inclusions, Chemical Geology 194 (2003) 41–49.

[11] O.V. Vasyukova, V.I. Fonarev, Experimental modeling of the transformation of $H_2O–CO_2–CH_4$ inclusions during isobaric cooling and isothermal compression, Geochemistry International 44 (2006) 1170–1180.

[12] L.W. Diamond, Review of the systematics of $CO_2–H_2O$ fluid inclusions, Lithos 55 (2001) 69–99.

[13] S.D. Malinin, The system $H_2O–CO_2$ at high temperatures and pressures, Geokhimiya 3 (1959) 235–245.

[14] A.J. Ellis, R.M. Golding, The solubility of carbon dioxide above 100 °C in water and in sodium chloride solutions, American Journal of Science 261 (1963) 47–60.

[15] S. Takenouchi, G.C. Kennedy, The solubility of carbon dioxide in NaCl solutions at high temperatures and pressures, American Journal of Science 263 (1965) 445–454.

[16] S. Takenouchi, G.C. Kennedy, The binary system $H_2O–CO_2$ at high temperatures and pressures, American Journal of Science 262 (1964) 1055–1074.

[17] K. Todheide, E.U. Franck, Das zweiphasengebiet und die kritische kurve im system kohlendioxid-wasser bis zu drucken von 3500 bar, Zeitschrift für Physikalische Chemie 37 (1963) 387–401.

[18] A.J. Ellis, The solubility of carbon dioxide in water at high temperatures, American Journal of Science 257 (1959) 217–234.

[19] S.E. Drummond, Boiling and mixing of hydrothermal fluids: chemical effects on mineral precipitation, Ph.D. Thesis, Pennsylvania State University, 1981.

[20] J.G. Blencoe, M.T. Naney, L.M. Anovitz, The $CO_2–H_2O$ system. III. A new experimental method for determining liquid–vapor equilibria at high subcritical temperatures, American Mineralogist 86 (2001) 1100–1111.

[21] J.G. Blencoe, The $CO_2–H_2O$ system. IV. Empirical, isothermal equations for representing vapor–liquid equilibria at 110–350 °C, $P ≤ 150$ MPa, American Mineralogist 89 (2004) 1447–1455.

[22] R.G. Sultanov, V.G. Skripka, A.Y. Namoit, Phase equilibrium and critical effect of water–methane system under increased temperature and pressure, Zhurnal Fizicheskoi khimi 46 (1972) 2160.

[23] L.C. Price, Aqueous solubility of methane at elevated pressures and temperatures, Aapg Bulletin-American Association of Petroleum Geologists 63 (1979) 1527–1533.

[24] K. Denbigh, The Principles of Chemical Equilibrium, Cambridge University Press, Cambridge, 1971.

[25] Z. Duan, N. Moller, J.H. Weare, An equation of state for the $CH_4–CO_2–H_2O$ system. I. Pure systems for 0 to 1000 °C and 0 to 8000 bar, Geochimica et Cosmochimica Acta 56 (1992) 2605–2617.

[26] Z. Duan, N. Moller, J.H. Weare, Prediction of methane solubilities in natural waters to high ionic strength from 0 to 250 °C and from 0 to 1600 bar, Geochimica et Cosmochimica Acta 56 (1992) 1451–1460.

[27] S. Mao, Z. Zhang, J. Hu, R. Sun, Z. Duan, An accurate model for calculating C_2H_6 solubility in pure water and aqueous NaCl solutions, Fluid Phase Equilibria 238 (2005) 77–86.

[28] W. Wagner, A. Pruss, International equation for the saturation properties of ordinary water substance. Revised according to the international temperature scale of 1990, Journal of Physical and Chemical Reference Data 22 (1993) 783–787 (Addendum to J. Phys. Chem. Ref. Data 16, 893 (1987)).

[29] K.I. Shmulovich, V.M. Shmonov, V.A. Mazur, A.G. Kalinichev, P–V–T and activity concentration relations in the $H_2O–CO_2$ system (homogeneous solutions), Geochemistry International 17 (1980) 123–139.

[30] C.E. Vanderzee, N.C. Haas, Second cross viral coefficients B12 for gas mixture (carbon dioxide + water) from 300 to 1000 K, Journal of Chemical Thermodynamics 13 (1981) 203–211.

[31] M.R. Patel, J.C. Holste, K.R. Hall, P.T. Eubank, Thermophysical properties of gaseous carbon dioxide–water mixtures, Fluid Phase Equilibria 36 (1987) 279–299.

[32] C.J. Wormald, M.J. Lloyd, Excess molar enthalpies for $(0.5H_2O + 0.5CO_2)$ at temperatures from 598.2 K to 698.2 K and pressures up to 20 MPa, Journal of Chemical Thermodynamics 26 (1994) 101–110.

[33] A.V. Plyasunov, E.L. Shock, Second cross viral coefficients for interactions involving water. Critical data compilation, Journal of Chemical and Engineering Data 48 (2003) 808–821.

[34] C. Tsonopouplos, An empirical correlation of second viral coefficient, AIChE Journal 20 (1974) 263–272.

[35] H. Hendl, E. Bich, E. Vogel, A new evaluation of (p, rho, T) measurements on steam with corrections for the effects of physical and chemical adsorption, Journal of Chemical Thermodynamics 29 (1997) 765–784.

[36] A.I. Abdulagatov, A.B. Kaplun, A.B. Meshalkin, I.M. Abdulagatov, G.V. Stepanov, Second caloric viral coefficients for real gases and combined spherical symmetric potential for simple molecular interactions, Journal of Chemical Thermodynamics 34 (2002) 2049–2072.

[37] D.M. Kerrick, G.K. Jacobs, A modified Redlich–Kwong equation for H_2O, CO_2, and $H_2O–CO_2$ mixtures at elevated pressures and temperatures, American Journal of Science 281 (1981) 735–767.

[38] J.A.D. Connolly, R.J. Bodnar, A modified Redlich–Kwong equation of state for $H_2O–CO_2$ mixtures: application to fluid inclusion studies (abstract), Transactions of the American Geophysics Union (EOS) 64 (1983) 350.

[39] N.F. Spycher, M.H. Reed, Fugacity coefficients of H_2, CO_2, CH_4, H_2O and of $H_2O–CO_2–CH_4$ mixtures: a viral equation treatment for moderate pressures and temperatures applicable to calculations of hydrothermal boiling, Geochimica et Cosmochimica Acta 52 (1988) 739–749.

[40] Z. Duan, N. Moller, J.H. Weare, An equation of state for the CH_4–CO_2–H_2O system. II. Mixtures from 50 to 1000 °C and 0 to 1000 bar, Geochimica et Cosmochimica Acta 56 (1992) 2619–2631.

[41] S.V. Churakov, M. Gottschalk, Perturbation theory based equation of state for polar molecular fluids. II. Fluid mixtures, Geochimica et Cosmochimica Acta 67 (2003) 2415–2425.

[42] X. Ji, S.P. Tan, H. Adidharma, M. Radosz, SAFT1-RPM approximation extended to phase equilibria and densities of CO_2–H_2O and CO_2–H_2O–NaCl systems, Industrial and Engineering Chemistry Research 44 (2005) 8419–8427.

[43] Z.H. Duan, Z.G. Zhang, Equation of state of the H_2O, CO_2, and H_2O–CO_2 systems up to 10 GPa and 2573.15 K: molecular dynamics simulations with ab initio potential surface, Geochimica et Cosmochimica Acta 70 (2006) 2311–2324.

[44] H. Teng, A. Yamasaki, M.K. Chun, H. Lee, Solubility of liquid CO_2 in water at temperatures from 278 K to 293 K and pressures from 6.44 MPa to 29.49 MPa and densities of the corresponding aqueous solutions, The Journal of Chemical Thermodynamics 29 (1997) 1301–1310.

[45] J.E. Garcia, Density of aqueous solutions of CO_2, in: Lawrence Berkeley National Laboratory Paper LBNL-49023, University of California, 2001.

[46] S. Bachu, J.J. Adams, Sequestration of CO_2 in geological media in response to climate change: capacity of deep saline aquifers to sequester CO_2 in solution, Energy Conversion and Management 44 (2003) 3151–3175.

[47] Y. Song, M. Nishio, B. Chen, S. Someya, T. Ohsumi, Measurement on CO_2 solution density by optical technology, Journal of Visualization 6 (2003) 41–51.

[48] N.N. Akinfiev, L.W. Diamond, Thermodynamic description of aqueous nonelectrolytes at infinite dilution over a wide range of state parameters, Geochimica et Cosmochimica Acta 67 (2003) 613–629.

[49] J.C. Tanger IV, H.C. Helgeson, Calculation of the thermodynamic and transport properties of aqueous species at high pressures and temperatures: revised equations of state for the standard partial molal properties of ions and electrolytes, American Journal of Science 288 (1988) 19–98.

[50] E.L. Shock, H.C. Helgeson, D.A. Sverjensky, Calculation of the thermodynamic and transport properties of aqueous species at high pressures and temperatures: standard partial molal properties of inorganic neutral species, Geochimica et Cosmochimica Acta 53 (1989) 2157–2183.

[51] E.L. Shock, H.C. Helgeson, Calculation of the thermodynamic and transport properties of aqueous species at high pressures and temperatures: standard partial molal properties of organic species, Geochimica et Cosmochimica Acta 54 (1990) 915–945.

[52] R. Crovetto, R.H. Wood, V. Majer, Densities of $\{xCO_2 + (1 - x)H_2O\}$ with $x < 0.014$ at supercritical conditions. Molar volumes, partial molar volumes of CO_2 at infinite dilution, and excess molar volumes, International Journal of Thermophysics 22 (1990) 231–243.

[53] G. Andersen, A. Probst, L. Murray, S. Butler, An accurate *PVT* model for geothermal fluids as represented by CO_2–H_2O–NaCl mixtures, in: The Seventeenth Workshop on Geothermal Reservoir Engineering, Stanford University, Stanford, CA, 1992, pp. 239–248.

[54] R.M. Enick, S.M. Klara, CO_2 solubility in water and brine under reservoir conditions, Chemical Engineering Communications 90 (1992) 23–33.

[55] E.R. Iglesias, S.L. Moya, An accurate formulation of the solubility of CO_2 in water for geothermal applications, in: The Seventeenth Workshop on Geothermal Reservoir Engineering, Stanford University, Standford, CA, 1992, pp. 231–238.

[56] Z.H. Duan, J.W. Hu, D.D. Li, S.D. Mao, Densities of the CO_2–H_2O and CO_2–H_2O–NaCl systems up to 647 K and 100 MPa, Energy & Fuels 22 (2008) 1666–1674.

[57] S.M. Sterner, R.J. Bodnar, Synthetic fluid inclusions. X. Experimental determination of P–T–V–X properties in the CO_2–H_2O system to 6 kb and 700 °C, American Journal of Science 291 (1991) 1–54.

[58] C.M. Destrigneville, J.P. Brodholt, B.J. Wood, Monte Carlo simulation of H_2O–CO_2 mixtures to 1073.15 K and 30 kbar, Chemical Geology 133 (1996) 53–65.

[59] J.G. Blencoe, J.C. Seitz, L.M. Anovitz, The CO_2–H_2O system. II. Calculated thermodynamic mixing properties for 400 °C, 0–400 MPa, Geochimica et Cosmochimica Acta 63 (1999) 2393–2408.

[60] R. Span, W. Wagner, On the extrapolation behavior of empirical equations of state, International Journal of Thermophysics 18 (1997) 1415–1443.

[61] L. Hnedkovsky, R.H. Wood, V. Majer, Volumes of aqueous solutions of CH_4, CO_2, H_2S and NH_3 at temperatures from 298.15 K to 705 K and pressures to 35 MPa, Journal of Chemical Thermodynamics 28 (1996) 125–142.

[62] W. Wagner, A. Pruß, The IAPWS formulation 1995 for the thermodynamic properties of ordinary water substance for general and scientific use, Journal of Physical and Chemical Reference Data 31 (2002) 387–535.

[63] R. Span, W. Wagner, A new equation of state for carbon dioxide covering the fluid region from the triple-point temperature to 1100 K at pressures up to 800 MPa, Journal of Physical and Chemical Reference Data 25 (1996) 1509–1596.

[64] U. Setzmann, W. Wagner, A new equation of state and tables of thermodynamic properties for methane covering the range from the melting line to 625 K at pressures up to 1000 MPa, Journal of Physical and Chemical Reference Data 20 (1991) 1061–1155.